Engineering Journal issn: 0125-8281

Article

Facile Fabrication of Chitosan/Starch Composite Films with Fumed Silica as an Additive

Krisana Siralertmukul[1,a], Nannalyn Yuenyaw[2,b], Supawin Watcharamul[2,c], and Roongkan Nuisin[2,d,*]

1 Metallurgy and Materials Research Institute, Chulalongkorn University, Bangkok 10330, Thailand
2 Department of Environmental Science, Faculty of Science, Chulalongkorn University, Bangkok 10330, Thailand
E-mail: [a]Krisana.S@Chula.ac.th, [b]Nannalyn.Y@gmail.com, [c]Supawin.W@Chula.ac.th, [d,*]Roongkan.N@Chula.ac.th (Corresponding author)

Abstract. Chitosan/cassava starch (CS/ST) composite films with different CS:ST (w/w) ratios were prepared by solution casting and investigated as a support for fumed silica ($fSiO_2$) dispersion. The CS, as a 1% (w/v) solution in 1% (w/v) acetic acid, and gelatinized ST, as a 3% (w/v) solution in 1% (w/v) acetic acid, were mixed at the appropriate volume ratios with a homogenizer, and then $fSiO_2$ at 1, 3, or 5% (w/w of CS) was added and cast as films. The morphology, tensile strength, contact angle, X-ray diffraction (XRD) pattern, and surface functional groups of the films were investigated. The external morphology of the CS/ST composite film revealed that the $fSiO_2$ particles were homogeneously dispersed into the polymer matrix. The water absorption and surface hydrophobicity of the composite film increased with increasing ST or CS contents. The hydrophobic acetyl groups of CS caused a notable reduction in the wettability as well as the water adsorption ability, which are preferable for a packaging film application. The CS/ST film with a high $fSiO_2$ content had a higher tensile strength due to the reinforcement effect of the $fSiO_2$ nanoparticles. The XRD patterns of the CS/ST films revealed that the 2θ of the crystalline region of CS were slightly changed when including the $fSiO_2$. The shift in the ST diffraction peak was probably due to the change in its chain orientation caused by hydrogen-bonding interactions between CS and ST molecules, resulting in their good adhesion.

Keywords: Cassava starch, chitosan, composite, films, fumed silica.

ENGINEERING JOURNAL Volume 25 Issue 9
Received 23 June 2021
Accepted 29 August 2021
Published 30 September 2021
Online at https://engj.org/
DOI:10.4186/ej.2021.25.9.45

1. Introduction

Chitosan (CS), 2-acetamido-2-deoxy-β-D-glucose, is a cationic semi-crystalline polysaccharide largely obtained from crustaceans, such as shrimp and crab shells, and produced by the N-deacetylation of chitin. The utility of marine by products is becoming a potential alternative for bio-based materials, due to their abundancy, low cost, non-toxic, and biodegradable [1,2]. The structure of chitosan is comprised of glucosamine units linked with β-(1,4) bonds [3]. In addition, chitosan contains a relatively large number of primary and secondary hydroxyl (-OH) and primary amine ($-NH_2$) groups, onto which various ligands can be easily attached [4]. Chitosan is soluble in dilute aqueous organic acids and insoluble in alkaline solutions and so can easily be formed into films and membranes by casting. The reactive functional groups of chitosan have been provided potential for covalent and ionic modifications allowing the improvement of its mechanical properties [5]. In view of the hydrophilicity, excellent film-forming ability, good mechanical properties, and high chemical reactivity of chitosan [1, 5], it is of interest as an alternative bio-based packaging material, and environmentally friendly packaging option for products. The biodegradable properties of chitosan make these films ideal candidates for various applications, such as affinity membranes, protective food coating, and food packaging purposes [6]. However, chitosan films have some disadvantages, including that they can be fragile when neutralized [7] and their unpleasant color affects the general appearance and consumer acceptance of their use in packaging.

Cassava starch (ST) is one of the most abundant agricultural products in Thailand. Starches are considered as one of the most promising biological polymers due to their abundant availability, renewability, biodegradability, and low cost [8-10]. Chemically, starch is a polysaccharide or a polymer of glucose. Structurally, starch has two forms, a straight chain of amylose and a branched chain of amylopectin. The α-1,4 linkages form the chains of glucose molecules and α-1,6 linkages occur at the branch points. However, pure starch is not suitable as a polymer for packaging materials due to its limited ability to form a thin film [11]. Starch films can be brittle and fragile, especially after the drying process. The addition of a plasticizer was found to enhance the brittleness and flexibility of starch films [12-14]. The presence of plasticizer is necessary in order to obtain a more rubbery-like material. The plasticizer can act as an internal lubricant to reduce the friction of the polymer chains. The free volume of the polymer matrix is increased when the plasticizer penetrates between the polymer chains. In general, plasticizers are compatible and miscible with the polymer matrix. Plasticizers, such as glycerol, ethylene glycol, and sorbitol, have been used for improving the physical and mechanical properties of CS films [15-17]. However, the water barrier and mechanical properties of plasticized-CS films with glycerol can change during storage [18].

The development of starch composite polymers by combining macromolecules with inorganic particles for improving some of their mechanical properties and increasing their applications has been reported [19, 20]. Fumed silica ($fSiO_2$), also known as pyrogenic silica or flame-hydrolyzed SiO_2, consists of microscopic amorphous SiO_2 fused into branched, chainlike, 3-dimensional (3D) secondary particles, which then agglomerate into tertiary particles [21]. Its properties of multihydroxy and high surface area. In literature is possible to find some studies dealing with chitosan/starch blends, the influence of the physico-chemical properties. Many studies indicated that $fSiO_2$ can improve and enhance the performance of polymeric materials for strength and thermal stability [22-24]. However, a relevant study on the starch modified by $fSiO_2$ has rarely been mentioned.

In the present study, chitosan/starch (CS/ST) composite films were prepared via solution casting. The CS/ST film with an optimum CS: ST ratio was selected as a support for $fSiO_2$ NPs. The correlation of the various $fSiO_2$ and CS contents to the physical, mechanical, and chemical properties of the CS/ST-$fSiO_2$ composite films was evaluated.

2. Materials and Methods

2.1. Materials

The CS derived from shrimp shells (commercial grade) with a degree of deacetylation of 81% and an average molecular weight (MW) of 200,000 kDa was obtained from Biolife Co. Ltd., Bangkok, Thailand. The ST (commercial grade, Plamangkorn, Bangkok, Thailand), had an ash content of 0.2%, starch content of 85%, and was used as received. The standardized, well-characterized $fSiO_2$ (CAS no. 112945-52-5, Cab-O-Sil™, Sigma, USA), used as an additive, had a particle diameter of about 0.014 nm, surface area of 200 ± 25 m^2/g, and density of 0.0368 g/cm^3. The glycerol (analytical grade) with a MW of 92.0938 g/mol and density of 1.261 g/cm^3 was from Suksaphan (Thailand) and used as a plasticizer.

2.2. Preparation of the CS/ST Films

First, the incorporation of glycerol in the CS/ST film was predetermined, where the addition of 20% (w/w) glycerol into the CS/ST films was chosen, because it supplied films with a better appearance and was easier to carry out (data not shown). For CS/ST film preparation, 1% (w/v) CS and 3% (w/v) ST solutions in 1% (w/v) acetic acid were prepared, the latter being gelatinized at 70 °C until a viscous solution was obtained. Then various (w/w) ratios of CS: ST (from 0:100 to 100:0) were mixed with stirring for 24 h to give a visually homogeneous solution. The solution was then filtered collecting the

filtrate. The CS/ST films were prepared by solution casting onto an acrylic mold (12.5 mm width × 16.5 mm length), dried at ambient temperature, neutralized with 1% (w/v) NaOH solution, and then rinsed and soaked with distilled water to remove the residual NaOH. For the CS/ST-fSiO_2 composites, fSiO_2 was added at 1, 3, or 5% (w/w of polymer) solution to the CS/ST mixture and then the films were cast and subsequently treated as per the CS/ST films above.

2.3. Characterization

2.3.1. Measurement of the physical properties

The thickness of the CS/ST film was measured using a flat parallel surface micrometer with a Vernier caliper (Mitutoya, Japan) and the average thickness calculated from five randomly selected points per specimen.

2.3.2. Measurement of the water contact angle (WCA)

The WCA measurements were performed using a contact angle meter. The films formed by the solution casting method had two surfaces with a different morphology. The surface contacting the acrylic mold was obviously smoother than the surface contacting with the air. Herein, all the values of the WCA for the CS/ST films were measured at the acrylic mold contact surface. A droplet of distilled water was dropped on the film surface. The WCA was measured on the side of water droplets and averaged from five droplets taken at different positions on the film surface. Calculation of the WCA was performed using a screen protractor software (http://www.iconico.com).

2.3.3. Water absorption

The dry weight (w_1) of each film (25.4 mm width × 76.2 mm length) was measured with an analytical balance. The film was dried in an oven at 50 °C for 24 h and then kept in a desiccator until use. The sample was immersed in distilled water for 24 h controlling the pH at 7. The film sample was then removed, excess water on its surface blotted off with filter paper, and the wet weight (w_2) of the sample was measured. The swelling property was calculated using Equation (1);

$$\text{Swelling (\%)} = [(w_2-w_1)/w_1] \times 100 \quad (1)$$

2.3.4. Tensile strength

The film was cut into slices of 150 mm (length) × 15 mm (width) and the tensile strength was determined using a universal testing machine (model Lloyd LR 100K, UK) on test specimens of 10 mm width and 20 mm gauge length. The tensile test specimens had a width of 10 mm and the tests were performed using a span length of 50 mm. The tensile tests were performed at a crosshead speed of 25 mm/min and a maximum load of 90 Newton, respectively. The average tensile stress at maximum load from five specimens was recorded.

2.3.5. External morphology

The external morphology of each respective CS/ST film was observed with scanning electron microscopy (SEM) using a model XL 30 CP (Phillips, The Netherlands) microscope. The films were cut, placed onto a brass stub and 50 Å gold vapor was sputtered onto the sample.

2.3.6. X-ray diffraction (XRD) analysis

The crystallinity of the polymer (cut into a small piece) was evaluated using XRD (Model PW3710 BASED, Philips Analytical, The Netherlands) operated with Cu Kα radiation (λ = 1.542 Å) at 40 kV and 30 mA. The XRD patterns were recorded in the reflection mode over an angular range of a 2θ of 10–30° at ambient temperature, scan time of 25 min, and scan speed of 0.040 (2θ s^{-1}).

2.3.7. Functional groups of CS/ST Film

The functional groups on the surface of the CS/ST films were analyzed using attenuated total reflectance - Fourier-transform infrared spectrometer (ATR-FTIR) using a model 1760× (Perkins Elmer, USA) instrument. The plasticized ST, CS, CS/ST films, and CS/ST-fSiO_2 composite films were cut into small pieces and the films scanned over a wavenumber range of 4000–650 cm^{-1}.

3. Results and Discussion

3.1. Physical and Surface Characterization

The transparent, homogeneous, thin, and flexible CS/ST films with 20% (w/w) glycerol plasticizer were obtained by solution casting. Visually, the polymeric films had a slightly yellow appearance increasing in intensity as the CS ratio increased, whereas increasing amounts of ST gave a paler yellow film. The average thickness of the plasticized-CS/ST films ranged from 0.02–0.04 mm (± 0.01 mm). The effect of the fSiO_2 content on the surface hydrophilicity of the films' surface and degree of swelling was revealed.

The surface wettability of the prepared films was determined by measurement of the WCA, where a WCA of more than 90° was designated as a hydrophobic film [25]. Increasing the amount of CS in the CS/ST film increased the WCA, reaching a WCA of nearly 80° at CS contents higher than 90% (w/w), as seen in Fig. 1. The amount of wetting was found to depend on the surface tension at the interface between the water droplet and the solid surface. The less hydrophilic solid surface of the CS/ST films with a high CS content gave a WCA close to 90°, which may be attributed to the hydrophobic

DOI:10.4186/ej.2021.25.9.45

backbone of the CS chains that contain acetyl groups. Increasing the amount of $fSiO_2$ in the CS/ST films increased the WCA. These results indicate that the wettability of the CS/ST film decreased with increasing $fSiO_2$ contents. Silica has a tunable surface comprised of hydrophilic silanol groups and moderately hydrophobic siloxane groups, which can be interchanged through thermal and chemical treatments [26]. In general, $fSiO_2$ is hydrophilic. Increasing, the $fSiO_2$ content from 1% to 3% and 5% (w/w) increased the WCA of the CS/ST-$fSiO_2$ composite films, indicating that the interaction of the CS molecules on the surface of SiO_2 became more hydrophobic and might have restricted the interaction between the silanol groups and water.

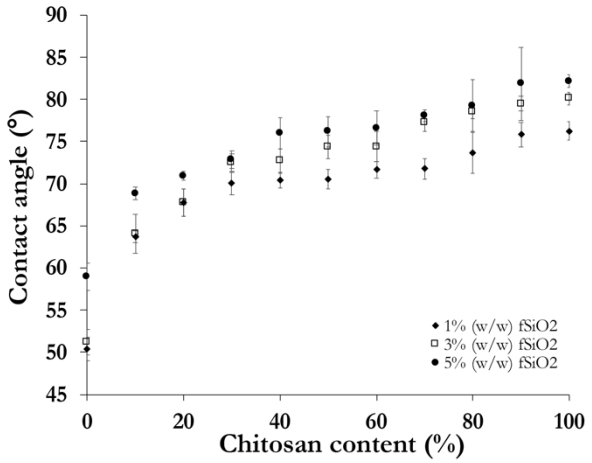

Fig. 1. Effect of the CS and $fSiO_2$ contents on the WCA of the CS/ST-$fSiO_2$ composite films. Data are shown as the mean ± SD derived from five measurements.

3.2. Absorption Properties

Figure 2 shows the percent swelling degree of the CS/ST-$fSiO_2$ films with increasing levels of CS and $fSiO_2$ contents. The degree of swelling decreased with increasing CS contents, which reflects the molecular structure of both polymers: CS contains hydrophobic acetyl groups while ST has hydrophilic hydroxyl groups. On the other hand, increasing the ST contents, and so increasing the density of hydroxyl groups to interact with water by hydrogen bonds (H-bonds), increased the swelling degree. Moreover, the inclusion of 20% (v/v) glycerol would have provided more hydroxyl groups to adsorb water molecules. Thus, the moisture affinity of the films was assisted by the glycerol molecules, as seen by the high compatibility with CS and enhanced mobility of the CS chains.

In general, polymer swelling degree depends upon its functional groups of polymer and osmotic pressure [27]. In the present work, increasing the amount of $fSiO_2$ NPs decreased the degree of swelling of the CS/ST films was decreased. It is possibly due to the H-bonds between the silanol groups on the $fSiO_2$ surface and the amino groups ($-NH_2$) of CS and/or hydroxyl groups (-OH) of ST seemed to affect the swelling property. This results in bonding formation, which acts as a barrier to restrict water penetration of CS/ST matrix. When water solvated the polymer chains it would limit their movement.

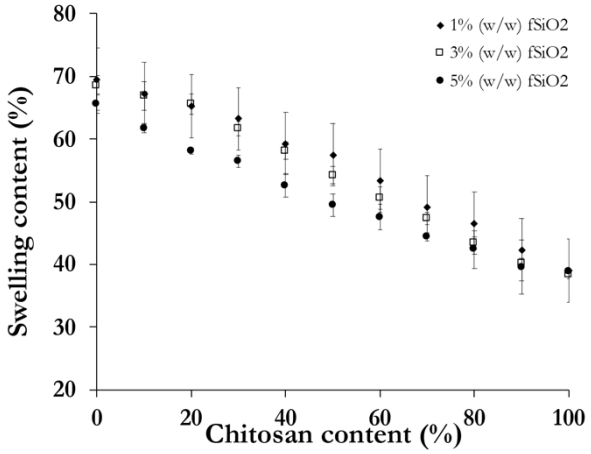

Fig. 2. Effect of the CS and $fSiO_2$ content on the swelling degree of CS/ST-$fSiO_2$ composite films. Data are shown as the mean ± SD derived from five measurements.

3.3. Mechanical Properties of the CS/ST Films

The tensile strength is a mechanical characteristic value for the evaluation of strength behavior and represents the maximum mechanical tensile strength that a film can be loaded with. Figure 3 shows the tensile strength of the CS/ST-$fSiO_2$ composite films with various CS: ST ratios and amounts of $fSiO_2$. High tensile strength values indicate the films are stronger with a high stress by bonding. The higher the ST amount the more brittle the films were. The tensile strength sharply decreased with increasing CS contents. A high CS content resulted in a tougher film, resulting from the crystalline structure of CS, as seen in the XRD analysis (section 3.4).

Increasing the content of $fSiO_2$ NPs gave higher tensile strength values supporting that the $fSiO_2$ NPs strongly influenced the polymer molecules. The CS chains were absorbed on $fSiO_2$ particles by (1) electrostatic attraction between the negative charges of SiO- on the $fSiO_2$ NPs and NH_3^+ of CS molecules, and (2) H-bonds between the hydroxyl and/or amino groups of CS (or ST) and silanol group of $fSiO_2$ [28]. These functional groups favor intramolecular H-bonding and restrict the CS chain movement. The addition of $fSiO_2$ NPs in the CS/ST polymer prevents intramolecular H-bonding and leads to the intermolecular bonds instead. The intermolecular interfacial adhesion is improved by the presence of intermolecular interactions between $fSiO_2$-ST or $fSiO_2$-CS in the CS/ST films [11]. When the $fSiO_2$ amount increased, the CS/ST film was reinforced by the $fSiO_2$ NPs and enhanced the film's mechanical properties. In addition, the tensile strength values were reduced with decreasing $fSiO_2$ contents.

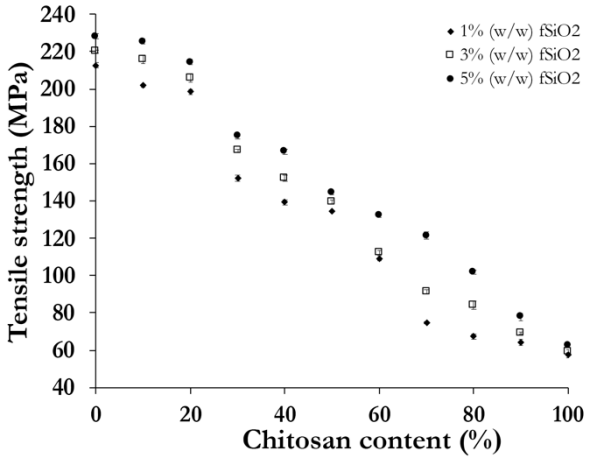

Fig. 3. Effect of the CS and $fSiO_2$ content on the tensile strength of CS/ST-$fSiO_2$ composite films. Data are shown as the mean ± SD derived from five measurements.

3.4. External Morphology of the CS/ST Films

Figure 4 shows SEM micrographs of the ST, CS, and CS/ST composite films. The apparent smooth surface of CS and ST films contrasts with the rough-grained appearance of the CS/ST composite films at 50:50 (w/w) ratio of CS: ST with 1% (w/w) $fSiO_2$. Increasing the $fSiO_2$ concentration led to a rougher surface of the CS/ST composite film, where the agglomeration of $fSiO_2$ particles became increasingly dense compared to that at a lower $fSiO_2$ content.

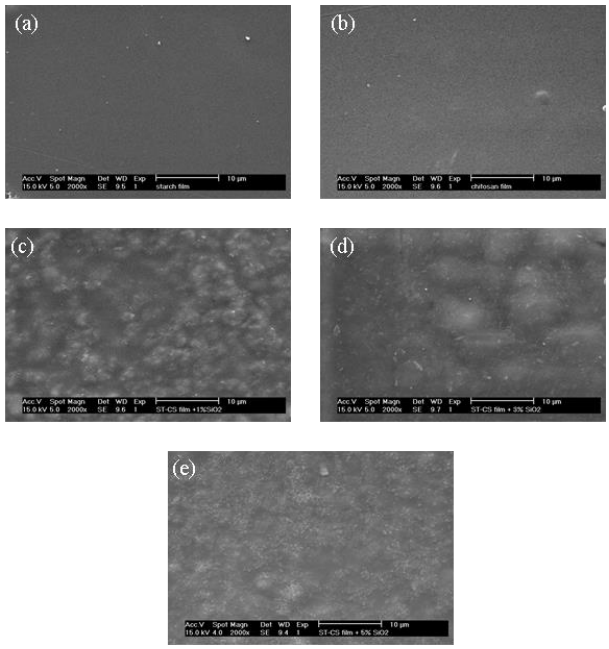

Fig. 4. Representative SEM micrographs (2,000 x magnification) of the (a) ST and (b) CS films, and the (c-e) CS/ST films with a $fSiO_2$ content of (c) 1, (d) 3, and (e) 5% (w/w).

3.5. Physical Structure of the CS/ST Films

Figure 5 shows the XRD patterns of the CS and CS/ST composite films. The native CS had three distinct crystallization peaks at a 2θ of 9.39°, 15.43°, and 20.63°. The high average MW CS revealed a high degree of crystallinity and intensity of diffraction peaks at a 2θ of 20.25°, and higher than at 9.39° (hydrated crystal peaks). In the ST film, the crystallinity could have originated from a clustered amylopectin structure, where the morphology of the crystalline part depends on the plant source [29]. The amylose structure was gelatinized which destroyed the A-style crystallinity. Therefore, the ST exhibited the B-style crystalline form at a 2θ of 5.6°, 15°, 17°, 22°, and 24° [30].

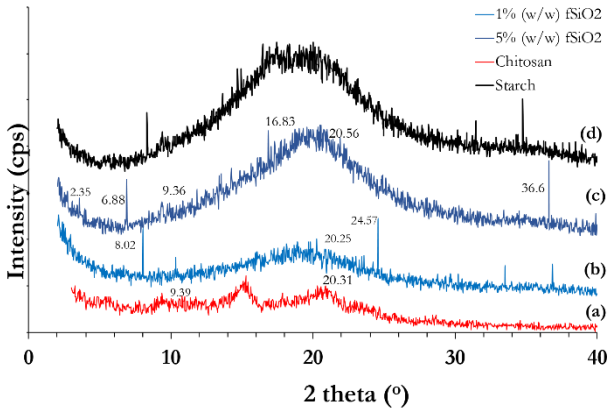

Fig. 5. Representative XRD traces of (a) pristine CS film; and (b, c) the CS/ST-$fSiO_2$ composite films with a $fSiO_2$ content of (b) 1% (w/w), (c) 5% (w/w), and (d) starch.

Figure 5(b) shows the CS/ST films with 1% (w/w) $fSiO_2$, revealing the diffraction peaks of CS and amylose at a 2θ of 20.25° and 24.57°, respectively. Increasing the $fSiO_2$ content to 5% (w/w of CS) shifted the diffraction peaks of CS to a 2θ of 9.38° and 20.25°. This shift in the diffraction peaks for CS and ST probably depends on the breaking of CS H-bonds with a minor microphase separation of the polymer. It has been reported that the X-ray patterns of a fresh potato starch film showed peaks for amylose at a 2θ of 5.5° and 17° [31], and the addition of glycerol at 20% (v/v) gave a sharper peak at 17°. The crystallization of starch could also have occurred due to amylose.

The plasticized-ST film with 20% (w/w) glycerol showed diffraction peaks at a 2θ of 5.76° and 14.96°, which was related to diffraction peaks of the free ST, as shown in Fig. 6(a). The shift in the diffraction patterns was due to the transportation of the plasticizer between the polymer molecules. In addition, the plasticized ST film with 20% (w/w) glycerol showed diffraction peaks at a 2θ of 9.6° and 19.53°, Fig. 6(b). The CS diffraction pattern appeared as a smaller peak than that of the plasticized-ST film, which was probably related to the chain orientation of the CS molecules being disturbed. CS is not completely

crystallized, as the crystalline domains by H- bonds and electrostatic interactions between the N-acetyl groups in which, some amorphous regions are also present [32].

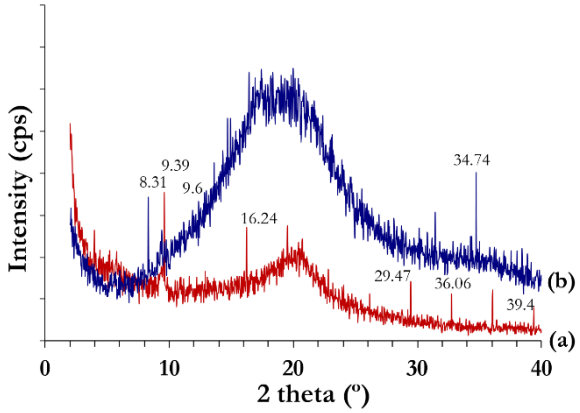

Fig. 6. Representative XRD traces of the (a) CS and (b) ST films, both plasticized with 20% (w/w) glycerol.

3.6. Characterization of the Surface Functional Groups of the CS/ST Films

Table 1 and Fig. 7 show the ATR-FTIR spectra of the ST, CS, and CS/ST composite films. For the ST film, the broad absorption bands at 3550–3200 cm^{-1} were ascribed to O-H stretching, while the strong absorption peaks at 2930 cm^{-1}, 1158 cm^{-1}, 1081 cm^{-1}, and 1015 cm^{-1} were from C-H (stretching) and C-O (stretching) [33]. The ATR-FTIR spectrum of CS showed strong absorption bands at 1158–1153 cm^{-1}, ascribed to the primary or secondary alcohol on the polysaccharide skeleton. The strong peaks at 1650–1580 cm^{-1} corresponded to NH_2 deformation vibration and the broad peak at 3450 cm^{-1} to -NH_2 symmetric stretching vibrations [34]. The strong peaks at 3600–3200 cm^{-1} were ascribed to C-H stretch vibration, and weak peaks at 2900–2800 cm^{-1} to the aliphatic carboxylic dimmer. The peaks at 1725–1700 cm^{-1} (strong) to -OH and CH deformation (ring), at 1420 cm^{-1} (medium) to C-H_2 stretching bending [35], at 1409 cm^{-1} (strong) to -OH stretch vibration, at 1383–1377 cm^{-1} (strong) to CH_3 deformation (bend), at 1267–1263 cm^{-1} (weak) to CH wag (ring) vibration, and at 1083 cm^{-1} (strong) to C-O stretching vibration. The other peaks were ascribed as the weak absorption at 1625–1500 cm^{-1} of COOH, C=O stretch and O-H deformation, and at 1560–1548 cm^{-1} for the NH_3^+ symmetric and asymmetric deformation vibration. The ATR-FTIR spectrum of the bulk $fSiO_2$ exhibited the broadband of ≡Si-OH at 3434 cm^{-1}, the strong vibration of Si-O at 1106 cm^{-1}, and Si-O asymmetric (medium) at 809 cm^{-1}. The crystallization sensitive zone was at 1106 cm^{-1}.

Figure 8 shows the ATR-FTIR spectra of the CS/ST-$fSiO_2$ composite films with CS: ST (w/w) ratios of 80:20, 60:40, 40:60, and 20:80 in the presence of 1% (w/w of CS) $fSiO_2$ NPs. The transmission peaks of -OH became wider and stronger with higher ST contents and were comprised of 3550–3200 cm^{-1} for O-H stretching and at 2930 cm^{-1} for CH stretching. The CS/ST composite films showed a combination of both CS's and ST's characteristics, but with shifts in the absorption peaks at wavenumber 1190–950 cm^{-1} (C-O stretching vibration).

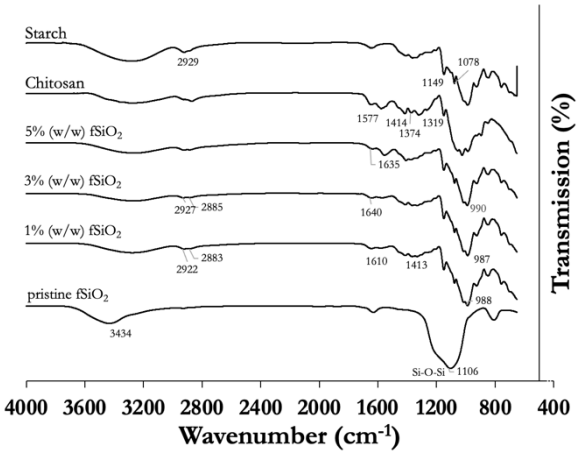

Fig. 7. Representative ATR-FTIR spectra of the ST, CS, CS/ST films with a 50:50 (w/w) ratio of CS: ST and a $fSiO_2$ content of 1, 3, and 5% (w/w of CS), and pristine $fSiO_2$.

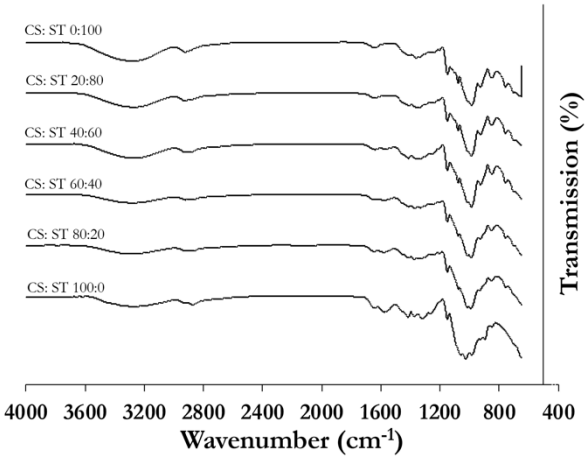

Fig. 8. Representative ATR-/FTIR spectra of the CS/ST films with various (w/w) ratios of CS: ST in the presence of 1% (w/w of CS) of $fSiO_2$.

4. Conclusion

Glycerol-plasticized CS/ST-$fSiO_2$ composite films were successfully prepared. The CS/ST films exhibited a deeper thickness with increasing ST amounts. Increasing the proportion of CS increased the WCA of the film. Increasing the CS content of the CS/ST film increased the WCA, due to the molecular orientation of CS that contains a hydrophobic acetyl group. Moreover, increasing the CS content decreased the degree of swelling and reduced the tensile stress at maximum load values of the CS/ST film. The mechanical properties of the CS/ST film could be improved by the addition of both CS and $fSiO_2$, giving a more flexible film due to the interaction of H-bonds of CS molecules (amino-to-amino groups or amino-to-hydroxyl group) being dominant. Increasing the $fSiO_2$ content

increased the WCA of the composite film due to the Si-OH group on the surface of SiO_2.

The ATR-FTIR spectra of CS/ST-fSiO_2 films revealed characteristic peaks of CS (-NH_2 at 1650–1580 cm^{-1}), ST (C-H stretching at 2930 cm^{-1}), and fSiO_2 (silanol group at 1106 cm^{-1}). The XRD diffraction pattern of the CS film revealed peaks at a 2θ of 9.39º, 15.43º, and 20.63º, while those for the CS/ST film were found at a 2θ of 20.25º, 9.38º, and 20.56º for 1, 3, and 5% (w/w) fSiO_2, respectively. The diffraction patterns of the amylose structure of ST were seen a 2θ of 24.57°. The crystallinity of ST and CS was shifted to a higher θ angle, which was possibly due to the orientation of polymer molecules where the interaction of CS and ST molecules tended to exhibit a microphase separation.

Table 1. Summary of the ATR-FTIR characteristics of the CS/ST composite films

Sample	Wavenumber (cm^{-1})	IR band assignment
Chitosan film		
Saccharide	905	Aliphatic aldehyde
	1153–158	strong; 1st or 2nd alcohol
Primary amine	1580–1650	NH_2 deformation
	3450	NH_2 symmetric stretch
Chitin (1st amide)	1322–1325	amide III: -OH and –CH deformation
	1515–1570	amide II: N-H deformation and C-N stretching
	1649–1655	Strong; amide I; C=O stretching
Other	1083	C-O stretching
	1263–1267	CH wag (ring)
	1377–1383	Strong; CH_3 deformation (bend)
	1420	OH and CH deformation (ring)
	1700–1725	Aliphatic carboxylic dimer
	2800–2900	C-H stretching
	3200–3600	OH stretch
	1409	-COOH C=O stretching and O-H deformation
	1548, 1560	NH_3^+ deformation, symmetric and asymmetric deformation
Starch film	1700–1725	-OH stretching
	2930	C-H stretching
	1158, 1081, and 1015	C-O stretching
fSiO_2	3434	≡Si-OH
	1106	Si-O

Acknowledgement

The authors acknowledge the Department of Materials Science, Faculty of Science, Chulalongkorn University for tensile strength measurement.

References

[1] E. Melro, F. E. Antunes, G. J. da silva, I. Cruz, P. E. Ramos, F. Carvalho, and L. Alves, "Chitosan films in food applications. Tuning film properties by changing acidic dissolution conditions," *Polymers*, vol. 13, no. 1, 2021.

[2] T. P. Singh, M. K. Chatli, and J. Sahoo, "Development of chitosan edible films: Process optimization using response surface methodology," *J. Food. Sci. Techol.* vol. 52, no. 5, pp. 2530-2543, 2015.

[3] F. Shahidi, J. Vidana Arachchi, and Y. J. Jeon, "Food applications of chitin and chitosans," *Trends Food Sci. Tech.,* vol. 10, no. 2, pp. 37-51, 1999.

[4] S. Islam, L. Arnold, and R. Padhye, "Comparison and characterisation of regenerated chitosan from 1-butyl-3-methylimidazolium chloride and chitosan from crab shells," *Biomed Res Int.*, vol. 2015, p. 874316, 2015.

[5] N. B. Boudouia, Z. Bengharez, and S. Jellali, "Preparation and characterization of chitosan extracted from shrimp shells waste and chitosan film: Application for Eriochrome black T removal from aqueous solutions," *Appl. Water Sci.,* vol. 9, no. 91, 2019.

[6] M. J. Bof, D. E. Locaso, and M. A. Garcia, "Corn starch-chitosan proportion affects biodegradable film performance for food packaging purposes," *Starch – Stärke*, vol. 73, 2021, Art. no. 2000104.

[7] N. E. Suyatma, L. Tighzert, and A. Copinet, "Effects of hydrophilic plasticizers on mechanical, thermal, and surface properties of chitosan films," *J. Agri. Food Chem.*, vol. 53, no. 10, pp. 3950-3957, 2005.

[8] A. Jiménez, M. J. Fabra, P. Talens, and A. Chiralt, "Edible and biodegradable starch films: A review," *Food Bioproc. Tech.*, vol. 5, no. 6, pp. 2058– 2076, 2012.

[9] A. Edhirej, S. M. Sapuan, M. Jawaid, N. I. Zahari, "Casava: Its polymer, fiber, composite, and application," *Polym. Compos.*, vol. 38, pp. 555-570, 2017.

[10] T. Jiang, Q. Duan, J. Zhu, H. Liu, and L. Yu, "Starch-based biodegradable materials: Challenges and opportunities," *KINGFA Sci.& Tech.* vol. 3, no. 1, pp. 8-18, 2020.

[11] H. Tang, H. Xiong, S. Tang, and P. Zou, "A starch-based biodegradable film modified by nano silicon dioxide," *J. Appl. Polym. Sci.*, vol. 113, no. 1, pp. 34-40, 2009.

[12] Q. P. Zhong and W. S. Xia, "Physicochemical properties of edible and preservative films from chitosan/cassava starch/gelatin blend plasticized with glycerol," *Food Tech. Biotech.,* vol. 46, no. 3, pp. 262-269, 2008.

[13] M. L. Sanyang, S. M. Sapuan, M. Jawaid, M. R. Ishak, and J. Sahari, "Effect of plasticizer typeand concentration on physical properties of biodegradable films based on sugar palm (*Arenga pinnata*) starch for food packaging," *J. Food. Sci Tech.,* vol. 53, no.1, pp. 326–336, 2016.

[14] P. M. Forsell, J. M. Mikkilä, G. K. Moates, and R. Parker, "Phase and glass transition behaviour of concentrated barley starch–glycerol–water mixtures, a model for thermoplastic starch," *Carbohydr. Polym.*, vol. 34, no. 4, pp. 275–282, 1997.

[15] Y. M. Navarro, K. Soukup, V. Jandova, M. M. Gomez, J. L. Solis, J. F. Cruz, R. Siche, O. Solcova, and G. J. F. Cruz, "Starch/chitosan/glycerol films produced from low-value biomass: effect of starch source and weight ratio on film properties," *J. Phys.: Conf. Ser.*, vol. 1173, p. 012008, 2019.

[16] N. Laohakunjit and A. Noomhorm, "Effect of plasticizers on mechanical and barrier properties of rice starch film," *Starch/Stärke*, vol. 56, pp. 348-356, 2004.

[17] M. G. N. Campos, L. H. I. Mei, and A. R. Santos Jr., "Sorbitol-plasticized and neutralized chitosan membranes as skin substitutes," *Mater. Res.*, vol. 18, no. 4, pp. 781-790, 2015.

[18] B. L. Butler, P. J. Vergano, R. F. Bunn, and J. L. Wiles, "Mechanical and barrier properties of edible chitosan films as affected by composition and storage," *J. Food. Sci.,* vol. 61, no. 5, pp. 953-955, 1996.

[19] P. M. Rahman, V. M. Abdul Mujeeb, and K. Muraleedharan, "Chitosan/nano ZnO composite films: Enhanced mechanical, antibacterial and dielectric properties," *Arab. J. Chem.*, vol. 11, pp. 120-127, 2018.

[20] J. H. R. Llanos and C. C. Tadini, "Preparation and characterization of bio-nanocomposite films based on cassava starch or chitosan, reinforced with montmorillonite or bamboo nanofibers," *Int. J. Biol. Macromol.*, vol. 107, pp. 371-382, 2017.

[21] O. Florke, B. Martin, L. Benda, S. Paschen, H. Bergna, W. Roberts, W. Welsh, M. Ettlinger, D. Kerner, and P. Kleinschmit, "Silica," in *Ullmann's Encyclopedia of Industrial Chemistry*. Weinheim, Germany: Wiley-VCH Verlag GmbH & Co., 2008.

[22] H. Zou, S. Wu, and J. Shen, "Polymer/silica nanocomposites: Preparation, characterization, properties, and applications," *Chem Rev.*, vol. 108, pp. 3893–957, 2008.

[23] S. Rimdusit, K. Punson, I. Dueramae, A. Somwangthanaroj, and S. Tiptipakorn, "Rheological and thermomechanical characterizations of fumed silica-filled polybenzoxazine nanocomposites," *Eng J.,* vol.15, no.3, pp. 27-38, 2011.

[24] M. S. Hussein and A. M. Fekry, "Effect of fumed silica/chitosan/ poly(vinylpyrrolidone) composite coating on the electrochemical corrosion resistance of Ti–6Al–4V alloy in artificial saliva solution," *ACS Omega*, vol. 4, no. 1, pp. 73-78, 2019.

[25] R. Forch, H. Schonherr, A. Tobias, and A. Jenkins "Contact angle goniometry," in *Surface Design: Applications in Bioscience and Nanotechnology,* R. Forch, H. Schonherr, A. Tobias, and A. Jenkins, Eds. Germany: Wiley-VCH Verlag GmbH & Co, 2009.

[26] A. M. Schrader, J. I. Monroe, R. Sheil, H. A. Dobbs, T. J. Keller, Y. Ki., S. Jain, M. S. Shell, J. N. Israelachvli, and S. Han, "Surface chemical heterogeneity modulated silica surface hydration," *Proc. Natl. Acad. Sci USA,* vol. 115, no. 12, pp. 2890-2895, 2018.

[27] S. Kumari, R. P. Singh, N. N. Chavan, S. V. Sahi, and N. Sharma, "Characterization of a novel nanocomposite film based on functionalized chitosan–Pt–Fe_3O_4 hybrid nanoparticles," *Nanomaterials,* vol. 11, p. 1275, 2021.

[28] T. Aubry, B. Largenton, and M. Moan, "Rheological study of fumed silica suspensions in chitosan solutions," *Langmuir,* vol. 15, no. 7, pp. 2380-2383, 1999.

[29] P. Le Bail, H. Bizot, and A. Buléon, "'B' to 'A' type phase transition in short amylose chains," *Carbohydr. Polym.*, vol. 21, no. 2-3, pp. 99-104, 1993.

[30] J. L. Jane, "Current understanding on starch granule structures," *J. Appl. Glycoscience,* vol. 53*,* no. 3, pp. 205-213, 2006.

[31] P. Myllarinen, A. Buleon, R. Lahtinen, and P. Forssell, "The crystallinity of amylose and amylopectin," *Carbohydr. Polym.,* vol. 48, pp. 41-48, 2002.

[32] M. Zienkiewicz-Strzalka, A. Derylo-Marczewska, Y. A. Skorik, V. A. Petrova, A. Choma, and I. Komaniecka, "Silver nanoparticles on chitosan/silica nanofibers: Characterization and antibacterial activity," *Int. J. Mol. Sci.*, vol 21, p. 166, 2020.

[33] R. J. Keller, *Sigma Library of FT-IR Spectra*. MO, USA: Sigma-Aldrich, Inc., 1986, vol. 1 & 2.

[34] X. Y. Wang, Y. M. Du, J. W. Luo, B. F. Lin, and J. F. Kennedy, "Chitosan/organic rectorite nanocomposite films: Structure, characteristic and drug delivery behaviour," *Carbohydr. Polym.,* vol. 69, pp. 41-49, 2007.

[35] N. Ardila, F. Daigle, M. C. Heuzey, A. Ajji, "Antibacterial activity of neat chitosan powder and flakes," *Molecules,* vol. 22, no. 1, p. 100, 2017.

Dr. Krisana Siralertmukul, photograph and biography not available at the time of publication.

Nannalyn Yuenyaw, photograph and biography not available at the time of publication.

Dr. Supawin Watcharamul, Supawin Watcharamul received his B.Sc. degree in General Science (Environmental Science) from Chulalongkorn University, Bangkok, Thailand, an M.Sc. degree in Environmental Science from Chulalongkorn University, Bangkok, Thailand, and a Ph.D. degree in Environmental Biotechnology from University of Newcastle upon Tyne, United Kingdom.
He has worked as a lecturer at the Department of Environmental Science, Faculty of Science, Chulalongkorn University, Bangkok, Thailand. In addition, he is teaching Biodegradation and Bioremediation and Environmental Toxicology for undergrads. Also, he is a committee of the M.Sc. and Ph.D. Programs in Biotechnology, Faculty of Science, Chulalongkorn University, Bangkok, Thailand. His research interests include soil microbial ecology, cellulosic biodegradation, and soil bioremediation of pollutants.

Dr. Roongkan Nuisin received her B.Sc. degree in Chemistry from Chiang Mai University, Thailand, in 1996, and M.Sc. degrees in Petrochemistry and Polymer Science, Chulalongkorn University, Thailand, in 1998 and a Ph.D. degree in Materials Science from Chulalongkorn University, Thailand, in 2002.
Since 2003, she has worked as a lecturer at Department of Department of Environmental Science, Faculty of Science, Chulalongkorn University. Her research interests include polymer synthesis, membrane emulsification and membrane technology, polymeric encapsulation, bio-based polymer for environmental applications.
She is an Associate Professor in Polymer Science.